

# Successive phase transition from superconducting to antiferromagnetic phase in $(\text{Ca}_6(\text{Al}, \text{Ti})_4\text{O}_y)\text{Fe}_2\text{As}_2$ studied via $^{75}\text{As}$ and $^{27}\text{Al}$ NMR

T. Nakano<sup>1</sup>, N. Fujiwara<sup>1\*</sup>, S. Tsutsumi<sup>1</sup>, H. Ogino<sup>2,3</sup>, K. Kishio<sup>2,3</sup> and J. Shimoyama<sup>2,3</sup>

<sup>1</sup> Graduate School of Human and Environmental Studies, Kyoto University,  
Yoshida-Nihonmatsu-cyo, Sakyo-ku, Kyoto 606-8501, Japan and

<sup>2</sup> Department of Applied Chemistry, The University of Tokyo, Tokyo 113-8656, Japan

<sup>3</sup> TRiP, Japan Science and Technology Agency (JST),  
Sanban-cho bldg. 5, Sanban-cho, Chiyoda-ku, Tokyo 102-0075, Japan

(Dated:)

An unusual successive phase transition from superconducting (SC) to antiferromagnetic (AF) phases was discovered via  $^{75}\text{As}$  and  $^{27}\text{Al}$  nuclear magnetic resonance (NMR) in  $(\text{Fe}_2\text{As}_2)(\text{Ca}_6(\text{Al}, \text{Ti})_4\text{O}_y)$  with four (Al, Ti)O layers intercalated between FeAs planes. Although the spatially-uniform AF ordering is clearly visible from  $^{27}\text{Al}$  spectra, the ordered moments are very small and the low-frequency fluctuation is much suppressed, contrary to existing pnictides with localized magnetic elements. Furthermore, the temperature ( $T$ ) dependence of the fluctuation at both nuclei is very similar throughout the entire temperature range. These facts suggest that some hybridization between Ti and Fe orbitals induces a uniform electronic state within FeAs and (Al, Ti)O layers accompanied by the SC and AF transitions. The iron-based pnictide with Ti-doped blocking layers is the first high- $T_c$  compound having metallic blocking layers.

PACS numbers: 74.70. Xa, 74.25. Dw, 74.25. nj, 76.60. -k

To date, a variety of iron-based pnictides have been discovered since the discovery of superconductivity in  $\text{LaFeAsO}_{1-x}\text{F}_x$  (La 1111 series).<sup>1</sup> Among these compounds, the 1111 series ( $R\text{FeAsO}_{1-x}\text{F}_x$   $R=\text{Ce}, \text{Pr}, \text{Sm}$ , etc. ) and the 122 series [ $\text{Ba}(\text{Fe}_{1-x}\text{Co}_x)_2\text{As}_2$ ] have been extensively studied because the highest superconducting transition temperature ( $T_c$ ) has been marked in the former family<sup>2,3</sup> and a large single crystal is available for the latter. The main difference between them is the distance between FeAs planes: The 0.8739 nm distance of the La 1111 series is greater than the 0.65 nm distance of the Ba 122 series.<sup>1,4,5</sup> Despite this  $\sim 0.22$  nm difference, their electronic phase diagrams completely differ from each other. For the 1111 series, an overlap of the stripe-type antiferromagnetic (AF) and superconducting (SC) phases is absent and the optimal  $T_c$  is realized away from the phase boundary, while for the 122 series, the two phases overlap and the optimal  $T_c$  is realized at the phase boundary.<sup>1-3,6-8</sup> The difference gives an impression that the two families are entirely different. However,  $\text{CaFe}_{1-x}\text{Co}_x\text{AsF}$  (Ca1111 series)<sup>9</sup> having an intermediate distance of 0.8593 nm was recently found to have an intermediate overlap,<sup>10</sup> suggesting that the phase diagrams show continuous variation depending on the distance between FeAs planes. The shrinkage of the distance increases the overlap, although the optimal  $T_c$  remains approximately the same among these compounds.

The question is what occurs in compounds having a large distance between FeAs planes. Actually, pnictides with perovskite-type blocking layers have a large distance of 1.3 – 2.5 nm.<sup>11</sup> A high  $T_c \sim 40$  K is

marked in these compounds. The highest  $T_c$  in this family has been marked at 47 K for a titanium oxide  $(\text{Fe}_2\text{As}_2)(\text{Ca}_4(\text{Mg}, \text{Ti})_3\text{O}_y)$ .<sup>12</sup> For other compounds, such as  $(\text{Fe}_2\text{As}_2)(\text{Ca}_5(\text{Sc}, \text{Ti})_4\text{O}_y)$  and  $(\text{Fe}_2\text{As}_2)(\text{Ca}_6(\text{Sc}, \text{Ti})_5\text{O}_y)$ ,  $T_c$  exceeds 40 K.<sup>11</sup> In  $(\text{Fe}_2\text{As}_2)(\text{Sr}_4(\text{Mg}, \text{Ti})_2\text{O}_6)$  and  $(\text{Fe}_2\text{As}_2)(\text{Sr}_4\text{V}_2\text{O}_6)$ ,  $T_c$  reaches 35 and 37 K, respectively.<sup>13,14</sup> This family is characterized by small lattice constants, a narrow As-Fe-As bonding angle, and a large distance between FeAs planes, which cause the lack of the hole pocket corresponding to the  $\alpha$  Fermi surface in undoped systems as theoretically investigated in  $(\text{Fe}_2\text{As}_2)(\text{Ca}_4\text{Al}_2\text{O}_6)$ .<sup>15,16</sup> Compounds such as  $(\text{Fe}_2\text{As}_2)(\text{Ca}_4\text{Al}_2\text{O}_6)$  and  $(\text{Fe}_2\text{As}_2)(\text{Sr}_4\text{Sc}_2\text{O}_6)$  are under the existing paradigm in the meaning that the blocking layers are insulators like other iron-based pnictides;<sup>15-17</sup> however Ti doping would induce new Fermi surfaces of Ti-orbital origin.<sup>18</sup> In  $(\text{Fe}_2\text{As}_2)(\text{Sr}_4\text{V}_2\text{O}_6)$ , the hybridization between V and Fe orbitals is possible, but strong correlations in V orbitals result in Mott-Hubbard-type insulating blocking layers.<sup>19,20</sup> The insulating blocking layers with localized magnetic moments has been suggested from the experiments using several techniques.<sup>21</sup>

For this family, the focus is on whether transition metals in blocking layers are involved in the formation of Fermi surfaces. An understanding would shed new light on the interplay between magnetism and superconductivity and high- $T_c$  mechanisms. We focus on  $(\text{Fe}_2\text{As}_2)(\text{Ca}_6(\text{Al}, \text{Ti})_4\text{O}_y)$  ( $y \sim 12$ ) with four (Al, Ti)O layers intercalated between FeAs planes, as shown in Fig. 1(a).<sup>22</sup> The series boasts of a 2.2 nm distance between FeAs planes. Isomorphic compounds with two and three (Al, Ti)O layers,  $(\text{Fe}_2\text{As}_2)(\text{Ca}_{n+2}(\text{Al}, \text{Ti})_n\text{O}_y)$  ( $n = 2, 3$ ) have also been synthesized; however, they are of an inferior quality than the four-layered samples.<sup>22</sup> The present compound is suitable for nuclear magnetic

\*Corresponding author: naoki@fujiwara.h.kyoto-u.ac.jp

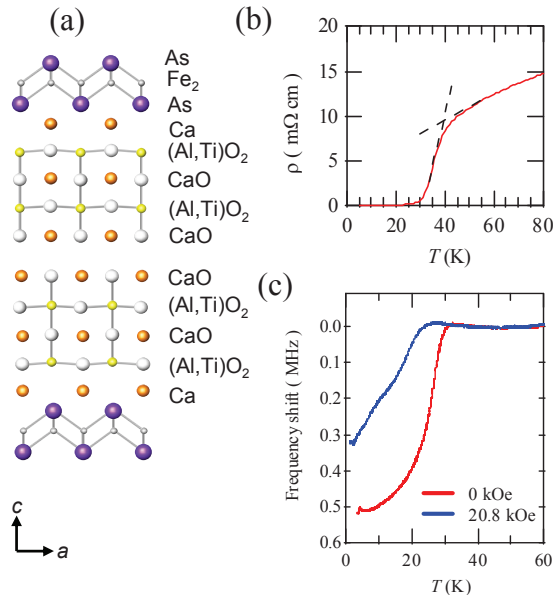


FIG. 1: (Color online) (a) Crystal structure of  $(\text{Fe}_2\text{As}_2)(\text{Ca}_6(\text{Al}, \text{Ti})_4\text{O}_y)$  [22]. (b) Temperature dependence of the resistivity. The onset of  $T_c$  is approximately 39 K [22]. (c) Detuning of a NMR coil measured at zero field and 20.8 kOe. The  $T_c$  value at 20.8 kOe is estimated to be  $23 \pm 5$  K. At this field,  $^{27}\text{Al}$ - $1/T_1T$  measurements were carried out, as shown in Fig. 3(d).

resonance (NMR) measurements because  $^{75}\text{As}$  ( $I = \frac{3}{2}$ ) and  $^{27}\text{Al}$  ( $I = \frac{5}{2}$ ) NMR can provide information about both FeAs and (Al, Ti)O layers on a microscopic level. We measured NMR using a conventional pulsed NMR method for powder samples. The chemical formula expected from the crystal structure is  $(\text{Fe}_2\text{As}_2)(\text{Ca}_6(\text{Al}_{0.5}\text{Ti}_{0.5})_4\text{O}_{12})$  in which Ti is formally nonmagnetic and therefore nonmagnetic blocking layers are expected.<sup>22</sup> A superstructure corresponding to some Al ordering was not observed from the x-ray analysis, implying that Al or Ti ions are randomly distributed in the blocking layers. The samples contained FeAs impurities, but the concentration was less than 2% in weight. The impurity phase was not observable in the  $^{75}\text{As}$  NMR measurements: it is known that FeAs exhibits a magnetic ordering at 70 K,<sup>23</sup> but we could not find any anomaly around 70 K in the  $^{75}\text{As}$  NMR measurements. Figure 1(b) shows the resistivity: The onset of  $T_c$  is estimated to be 39 K and zero resistivity is at approximately 30 K, which is approximately the same as  $T_c$  determined from the detuning of an NMR tank circuit at 36.8 MHz, as shown in Fig. 1(c).

Figures 2(a) and 2(b) show field-swept  $^{75}\text{As}$  and  $^{27}\text{Al}$  NMR spectra, respectively, measured from spin-echo intensity at 45.1 MHz. The  $^{75}\text{As}$  NMR spectra for the central transition ( $I = -1/2 \leftrightarrow 1/2$ ) broaden because of the second-order quadrupole effect similar to other iron-based pnictides. At first glance, the spectral pattern with four bumps is suggestive of two  $^{75}\text{As}$  sites having differ-

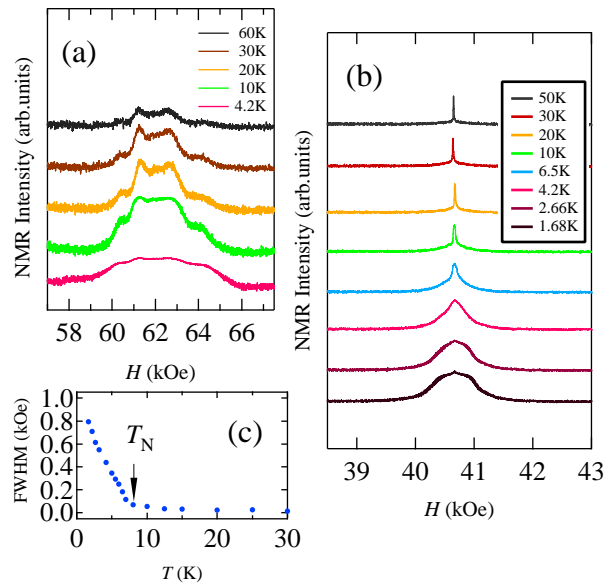


FIG. 2: (Color online) (a)  $^{75}\text{As}$  NMR spectra at 45.1 MHz. The broadening at 4.2 K shows the appearance of some spin ordering. (b)  $^{27}\text{Al}$  NMR spectra at 45.1 MHz. A rectangular-type powder pattern implies the appearance of spatially uniform AF moments. (c) The linewidth of  $^{27}\text{Al}$  NMR spectra. The ordering temperature is 7 K.

ent electric field gradients (EFGs). In this case, however, the intensity difference between two  $^{75}\text{As}$  sites is not explained. Instead, the lineshape is well reproduced by considering a large anisotropic coefficient ( $\eta$ ) of EFG. The pure quadrupole frequency ( $\nu_Q$ ) and  $\eta$  are estimated to be  $\nu_Q = 13.4$  MHz and  $\eta \sim 0.6$ , respectively. The large  $\eta$  value is rare in iron-based pnictides, although a fairly large  $\eta$  ( $\sim 0.3$ ) has been reported in  $\text{CaFe}_{1-x}\text{Co}_x\text{AsF}$ .<sup>10</sup> Two bumps around 61 and 63 kOe correspond to  $\theta = 90^\circ$  and  $42^\circ$ , respectively, where  $\theta$  represents the angle between the  $c$  axis and the applied field. The lineshape changes at low temperatures reflecting some spin ordering. However, the position of the low-field bump is unchanged even in the ordered state, implying that the ordered moments are aligned parallel to FeAs planes like other pnictides: For the samples associated with the low-field bump, the stripe-type ordered moments result in the internal field perpendicular to the applied field, and have no effect on the low-field bump. The appearance of some ordering is clearly visible from the  $^{27}\text{Al}$  NMR spectra. Although satellite signals ( $I = \pm\frac{3}{2} \leftrightarrow \pm\frac{5}{2}$ ) are expected to appear because of the quadrupole effect, only a sharp signal is observable at high temperatures, implying that Al nuclei experience an EFG that is very small and is somewhat distributed. The sharp signal also indicates that the local environment around  $^{27}\text{Al}$  is hardly affected by random Al distribution. The sharp signal changes to a rectangular-type powder pattern at low temperatures. The ordering temperature ( $T_N$ ) is estimated to be 7 – 8

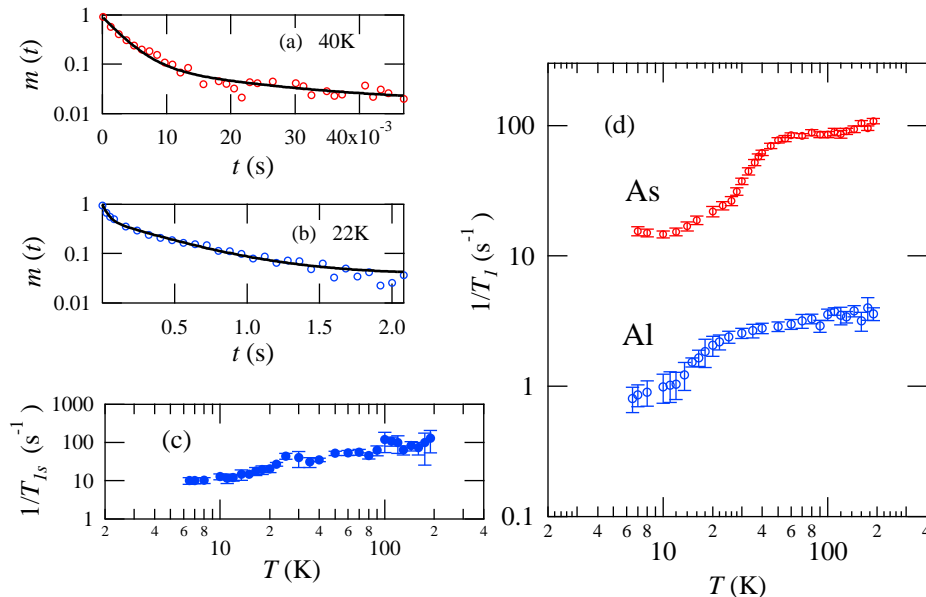


FIG. 3: (Color online) (a) Recovery curve,  $m(t) = 1 - M(t)/M(\infty)$  of  $^{75}\text{As}$ . Data are fitted by Eq. (1). (b) Recovery curve of  $^{27}\text{Al}$ . Data are fitted by Eq. (2). (c) Temperature dependence of the fast-recovery component  $1/T_{1s}$  [See Eq. (2)]. (d) Temperature dependence of  $1/T_1$  for  $^{75}\text{As}$  and  $^{27}\text{Al}$ .

K from the temperature ( $T$ ) dependence of the linewidth, as shown in Fig. 2(c). The tail of the rectangular pattern on both sides is caused by the effect of small satellite signals. The rectangular-type powder pattern is symmetric with regard to the free position corresponding to the Larmor frequency, demonstrating that an AF spin configuration is formed and the amplitude of spin moments is spatially uniform.

Relaxation rates ( $1/T_1$ ) of  $^{75}\text{As}$  and  $^{27}\text{Al}$  were measured using a saturation-recovery method. We measured  $1/T_1T$  of  $^{75}\text{As}$  ( $(1/T_1T)_{As}$ ) at the lower-field bump and  $1/T_1T$  of  $^{27}\text{Al}$  ( $(1/T_1T)_{Al}$ ) at a low field of 20.8 kOe because a large field could potentially break down the superconductivity or reduce the SC volume fraction. Prior to the measurements, we confirmed whether the superconductivity is maintained at 20.8 kOe from the detuning [Fig. 1(c)]. At this field,  $T_c$  is estimated to be  $23 \pm 5$  K. The decrease in  $T_c$  was also confirmed from the AC and DC susceptibility.<sup>24</sup> A remarkable decrease in  $T_c$  under a low field may be a peculiarity of this system. Such caution is not required for  $^{75}\text{As}$ , because FeAs planes at the low-field bump are parallel to the applied field, and the decrease in  $T_c$  under the field is neglected. Figures 3(a) and 3(b) show recovery curves, time variations of spin-echo intensity after a saturation pulse, for  $^{75}\text{As}$  and  $^{27}\text{Al}$ , respectively. Data of  $^{75}\text{As}$  follow the conventional rate equation for the central transition ( $I = -1/2 \leftrightarrow 1/2$ ),

$$1 - \frac{M(t)}{M(\infty)} = 0.9\exp(-6t/T_1) + 0.1\exp(-t/T_1), \quad (1)$$

while all  $^{27}\text{Al}$  satellite signals are saturated owing to the small quadrupole splitting, and data of  $^{27}\text{Al}$  exhibit a recovery with two components,

$$1 - \frac{M(t)}{M(\infty)} = (1 - c)\exp(-t/T_{1s}) + c\exp(-t/T_1). \quad (2)$$

The  $T$  dependence of the fast- and slow-recovery components is shown in Figs. 3(c) and 3(d), respectively, together with  $(1/T_1T)_{As}$ . The value of  $c$  increases approximately linearly from 0.4 to 0.6 with increasing temperature. The fast-recovery component  $1/T_{1s}$  hardly reflects the electronic state, and possibly originates from the nuclear spin diffusion. Bending points in Fig. 3(d) are in good agreement with  $T_c$  determined from the detuning in Fig. 1(c).  $1/T_1$  values of  $^{75}\text{As}$  are one order greater than those of  $^{27}\text{Al}$ , while the  $T$  dependence, excluding  $T_c$  values, of both nuclei is very similar. The  $T$  dependence of  $(1/T_1T)_{As}$  and  $(1/T_1T)_{Al}$  normalized by the values at  $T_c$  is shown in Fig. 4(a). They both show Curie-Weiss behavior and are almost the same at high temperatures above  $T_c$ , implying that both nuclei experience the same spin fluctuation.

Interestingly, Curie-Weiss behavior returns in  $1/T_1T$  at low temperatures, reflecting the AF ordering. The question is which of Ti and Fe is responsible for the AF ordering. In the existing paradigm, the blocking layers are insulators and the AF ordering would occur either in FeAs or (Al, Ti)O layers. In both cases, some of the results are not well explained.

(1) In the case of Fe origin, Fe orbitals are responsible for both SC and AF orderings, which would be very

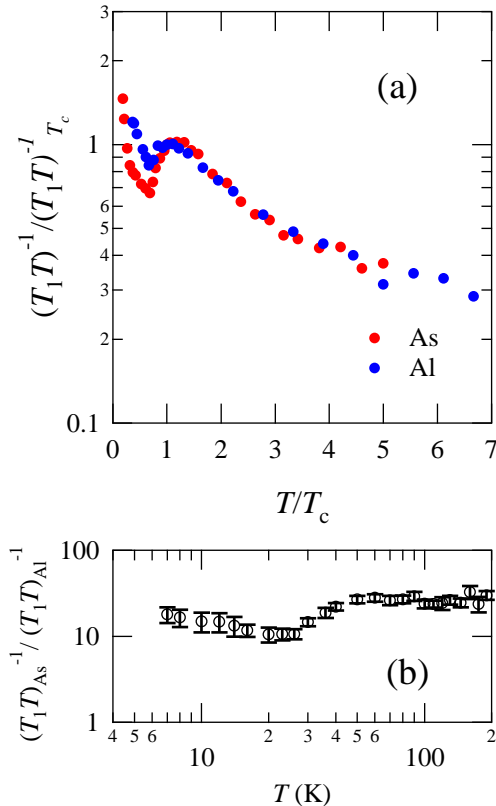


FIG. 4: (Color online)(a) Plot of  $1/T_1 T$  versus  $T$  normalized by those at  $T_c$ . (b) The ratio of  $(1/T_1 T)_{As} / (1/T_1 T)_{Al}$ . The values are almost the same except for the temperature range between 20 and 40 K corresponding to  $T_c$  values at zero field and 20.8 kOe.

exotic if possible. The possibility is ruled out because two inner (Al, Ti)O layers are away from FeAs planes and only weak dipole coupling is effective as hyperfine coupling, making the linewidth narrow and the spectral weight strong at the central position of the  $^{27}\text{Al}$  line-shape. The linewidth of  $^{27}\text{Al}$  in the inner (Al, Ti)O layers is estimated as  $\sim 5$  Oe when a Bohr magneton is assumed as the amplitude of Fe moments.

(2) In the case of localized Ti moments, the appearance of the spatially uniform AF spin moments results in a  $3d^1$  state having an electron at each Ti site, despite that Ti ions are expected to be nonmagnetic from the crystal structure. Such case may be possible when electrons are transferred from FeAs planes to (Al, Ti)O layers. If all Ti ions were magnetic, Al nuclei would experience strong low-frequency fluctuation, considering the location of Al nuclei. This is seen in other compounds such as  $\text{SmFeAsO}_{1-x}\text{F}_x$  and  $\text{NdFeAsO}_{1-x}\text{F}_x$ : Predominant spin fluctuation, namely Curie-Weiss behavior in  $1/T_1$ , masks information from FeAs planes.<sup>25,26</sup> On the contrary,  $1/T_1$  is almost constant at  $^{27}\text{Al}$ , and  $T_c$  is observable at high temperatures in the present compound.

Experimental results are not perfectly explained by the

existing paradigm. The reason why (Al, Ti)O layers are not insulators is derived directly from the amplitude of the ordered moments  $\langle S_i \rangle$ . The amplitude is estimated from the hyperfine coupling  $^{27}A_{hf}$  and internal field  $\Delta H$  of  $^{27}\text{Al}$  as  $\Delta H = g\mu_B \langle S_i \rangle^{27} A_{hf}$ . The coupling  $^{27}A_{hf}$  mainly originates from the Fermi contact rather than the super-transferred hyperfine coupling. Because the coupling is rather isotropic, all fluctuations are observable at  $^{27}\text{Al}$  sites, but in-plane AF fluctuations would be predominant as investigated in the 122 series.<sup>27</sup> In the case of  $^{75}\text{As}$ , the hyperfine coupling  $^{75}A_{hf}$  mainly originates from the transferred hyperfine coupling. As nuclei experience the in-plane AF fluctuations remarkably when the field is applied parallel to FeAs planes.<sup>27</sup> Therefore, the in-plane AF fluctuations would be predominant at both  $^{27}\text{Al}$  and  $^{75}\text{As}$  sites. The coupling  $^{27}A_{hf}$  can be estimated by the following relation assuming that both  $^{27}\text{Al}$  and  $^{75}\text{As}$  experience the same AF fluctuation:

$$\frac{1}{(T_1)_{As}} / \frac{1}{(T_1)_{Al}} \sim \left( \frac{^{75}\gamma_N}{^{27}\gamma_N} \right)^2 \left( \frac{^{75}A_{hf}}{^{27}A_{hf}} \right)^2. \quad (3)$$

The value is approximately 30 at high temperatures, as seen in Fig. 4(b). The gyromagnetic ratios of  $^{75}\text{As}$  and  $^{27}\text{Al}$ ,  $^{75}\gamma_N$  and  $^{27}\gamma_N$  are 7.29 and 11.09 MHz/10 kOe, respectively. The coupling  $^{75}A_{hf}$  has been estimated to be 26 kOe/ $\mu_B$  for the field parallel to the FeAs planes,<sup>27</sup> and  $^{27}A_{hf}$  is estimated to be 3.1 kOe/ $\mu_B$  from Eq. (3). The internal field  $\Delta H$  is  $\sim 0.3 - 0.4$  kOe as seen in Fig. 2(b), therefore  $\langle S_i \rangle$  is estimated to be  $\sim 0.05 - 0.07$ . The value is very small compared with that expected from localized spin moments  $\langle S_i \rangle = 1/2$ . The small AF magnetization is a feature of weakly antiferromagnetic metals. To explain the small amplitude of  $\langle S_i \rangle$  and the similarity between  $^{75}\text{As}$  and  $^{27}\text{Al}$  sites in  $1/T_1T$  [Fig. 4(b)],<sup>28</sup> some hybridization between Ti and Fe orbitals would be crucial.

For  $(\text{Fe}_2\text{As}_2)(\text{Sr}_4\text{V}_2\text{O}_6)$  with a high  $T_N$  of 150 K,<sup>29</sup> V orbitals should be removed from the Fermi level owing to strong correlations of  $d$  orbitals in vanadium; namely a Mott-Hubbard-type insulating state is realized. Taking account of a small  $T_N$  ( $\sim 7$  K) caused by Al-rich doping, correlations are expected to be small, and therefore, (Al, Ti)O layers are responsible for Fermi surfaces, contrary

to the VO blocking layers. The appearance of the AF state following the SC state implies that some parts of the Fermi surfaces are not involved in the formation of a SC gap. In this sense, the phenomenon is similar to homogeneous coexistence of the incommensurate spin density wave and superconductivity in the crossover regime of the 122 or 1111 series.<sup>30–32,10</sup>

In summary, an unusual successive phase transition from the SC to AF phases was observed via  $1/T_1T$ . Although the spatially uniform AF ordering is clearly visible from  $^{27}\text{Al}$  spectra, localized spin moments are unlikely to exist in (Al, Ti)O blocking layers. The ordered moments are very small, and the  $T$  dependence of  $1/T_1T$  at both  $^{75}\text{As}$  and  $^{27}\text{Al}$  sites is very similar throughout the entire temperature range. These facts suggest that some hybridization between Ti and Fe orbitals induces a uniform electronic state within FeAs and (Al, Ti)O layers accompanied by the SC and weak AF transitions.

The authors would like to thank K. Kuroki for discussion. The present work was partially supported by a Grant-in-Aid (Grant No. KAKENHI 23340101) from the Ministry of Education, Science, and Culture, Japan.

- 
- <sup>1</sup> Y. Kamihara *et al.*, J. Am. Chem. Soc. **130**, 3296 (2008).  
<sup>2</sup> Y. Kamihara *et al.*, N. J. Phys. **12**, 033005 (2010).  
<sup>3</sup> C. Hess *et al.*, Europhys. Lett. **87**, 17005 (2009).  
<sup>4</sup> M. Rotter *et al.*, Phys. Rev. B **78**, 020503(R) (2008).  
<sup>5</sup> A. S. Sefat *et al.*, Phys. Rev. Lett. **101**, 117004 (2008).  
<sup>6</sup> C. Lester *et al.*, Phys. Rev. B **79**, 144523 (2009).  
<sup>7</sup> F. Rullier-Albenque *et al.*, Phys. Rev. Lett. **103**, 057001 (2009).  
<sup>8</sup> S. Nandi *et al.*, Phys. Rev. Lett. **104**, 057006 (2010).  
<sup>9</sup> S. Matsuiishi *et al.*, J. Am. Chem. Soc. **130**, 14429 (2008).  
<sup>10</sup> T. Nakano *et al.*, Phys. Rev. B **83**, 180508(R) (2011).  
<sup>11</sup> H. Ogino *et al.*, Appl. Phys. Lett. **97**, 072506 (2010).  
<sup>12</sup> H. Ogino *et al.*, Appl. Phys. Express **3**, 063103 (2010).  
<sup>13</sup> S. Sato *et al.*, Supercond. Sci. Technol. **23**, 045001 (2010).  
<sup>14</sup> X. Zhu *et al.*, Phys. Rev. B **79**, 220512(R) (2009).  
<sup>15</sup> T. Miyake *et al.*, J. Phys. Soc. Jpn **79**, 123713 (2010).  
<sup>16</sup> H. Usui and K. Kuroki, Phys. Rev. B **84**, 024505 (2011).  
<sup>17</sup> I. R. Shein and A. L. Ivanovskii, Phys. Rev. B **79**, 245115 (2009).  
<sup>18</sup> I. R. Shein and A. L. Ivanovskii, Cent. Eur. J. Phys. **8**, 432 (2010).  
<sup>19</sup> I. I. Mazin, Phys. Rev. B **81**, 020507(R) (2010).  
<sup>20</sup> H. Nakamura and M. Machida, Phys. Rev. B **82**, 094503 (2010).  
<sup>21</sup> S. Tatematsu *et al.*, J. Phys. Soc. Jpn. **79**, 123712 (2010).  
<sup>22</sup> H. Ogino *et al.*, Supercond. Sci. Technol. **23**, 115005 (2010).  
<sup>23</sup> K. Segawa and Y. Ando, J. Phys. Soc. Jpn. **78**, 104720 (2009).  
<sup>24</sup> A. Hisada *et al.*, private communication.  
<sup>25</sup> G. Prando *et al.*, Phys. Rev. B **81**, 100508(R) (2010).  
<sup>26</sup> P. Jeglič *et al.*, Phys. Rev. B **79**, 094515 (2009). The data for  $1/T_1$  are shown in arXiv:086.1450 [v1].  
<sup>27</sup> K. Kitagawa, *et al.*, J. Phys. Soc. Jpn. **77**, 114709 (2008).  
<sup>28</sup> In Fig. 4 (b), the comparison of  $1/T_1T$  measured at different  $T_c$  values is presented for experimental restrictions. If  $^{27}\text{Al}$  NMR measurements were carried out at an extremely small applied field, the similarity between  $(1/T_1T)_{\text{Al}}$  and  $(1/T_1T)_{\text{As}}$  would be seen throughout the entire  $T$  range.  
<sup>29</sup> G. Cao, *et al.*, Phys. Rev. B **82**, 104518 (2010).  
<sup>30</sup> M. H. Julien *et al.*, Europhys. Lett. **87**, 37001 (2009).  
<sup>31</sup> Y. Laplace *et al.*, Phys. Rev. B **80**, 140501(R) (2009).  
<sup>32</sup> P. Marsik *et al.*, Phys. Rev. Lett. **105**, 057001 (2010).